





Artificial Photosynthesis

Zitierweise:

Internationale Ausgabe: doi.org/10.1002/anie.202003278

Deutsche Ausgabe: doi.org/10.1002/ange.202003278

Characterization of the Fe^V=O Complex in the Pathway of Water Oxidation

Roman Ezhov, Alireza Karbakhsh Ravari, and Yulia Pushkar*

Abstract: Hypervalent $Fe^{V}=O$ species are implicated in a multitude of oxidative reactions of organic substrates, as well as in catalytic water oxidation, a reaction crucial for artificial photosynthesis. Spectroscopically characterized Fe^V species are exceedingly rare and, so far, were produced by the oxidation of Fe complexes with peroxy acids or H_2O_2 : reactions that entail breaking of the O-O bond to form a $Fe^V = O$ fragment. The key $Fe^V = O$ species proposed to initiate the O-O bond formation in water oxidation reactions remained undetected, presumably due to their high reactivity. Here, we achieved freeze quench trapping of six coordinated $[Fe^V = O, (OH)(Pytacn)]^{2+}$ (Pytacn = 1-(2'-pyridylmethyl)-4,7dimethyl-1,4,7-triazacyclononane) (2) generated during catalytic water oxidation. X-ray absorption spectroscopy (XAS) confirmed the Fe^V oxidation state and the presence of a $Fe^V=0$ bond at ≈ 1.60 Å. Combined EPR and DFT methods indicate that **2** contains a S = 3/2 Fe^V center. **2** is the first spectroscopically characterized high spin oxo-Fe^V complex and constitutes a paradigmatic example of the $Fe^V = O(OH)$ species proposed to be responsible for catalytic water oxidation reactions.

Enzymatic high-valent oxo-iron species have been selected by Nature to conduct challenging oxidative reactions such as aliphatic C—H bond oxidation.^[1] These reactions have been successfully mimicked using Fe^V=O and Fe^{IV}=O synthetic models.^[2] For a water oxidation reaction, however, Nature relies on a Mn₄Ca cluster inside the Photosystem II protein.^[3] To date, the most extensive mimic of that process was achieved with Ru based water oxidation catalysts.^[4] However, first row transition metals and especially Fe based water oxidation catalysts carry a great promise as they utilize earth abundant elements.^[5]

An example of a notably durable Fe-based water oxidation catalyst is $[Fe(Pytacn)(OTf)_2]$ (Pytacn = 1-(2'-pyridyl-methyl)-4,7-dimethyl-1,4,7-triazacyclononane and OTf = -SO₃CF₃) (1), which catalyzes the water oxidation reaction using Ce^{IV} (Cerium, ammonium nitrate, CAN) or NaIO₄ as oxidants. DFT calculations proposed that the reaction proceed via a high spin (S = 3/2) $[Fe^V = O,(OH)(Pytacn)]^{2+}$ (2) intermediate [5c] (Figure 1). Previously, 2 was not detected spectroscopically but was computationally shown to be energetically accessible and reactive with water via water

nucleophilic attack on the Fe^V=O fragment in the rate determining step.^[5c] Follow up spectroscopic experiments did not identify spectroscopic signatures of **2** in the reaction mixtures, suggesting that this species must be very short lived. Fe^V (d³) is isoelectronic to Ru^V (d³): the species which are also very short lived but can be observed in situ at selected conditions.^[4b,c,6] Moreover, depending on the reaction conditions, Ru^V=O species can form the O–O bond via both radical coupling (RC)^[7] and water nucleophilic attack (WNA) pathways.^[4c,6b] Current experiments show that [Fe^V=O,(OH) (Pytacn)]²⁺ reacts with water via WNA on the oxo ligand, assisted by an initial hydrogen bond interaction of the water molecule with the *cis*- positioned hydroxide ligand.^[5d]

X-ray absorption spectroscopy (XAS) is a sensitive technique for the analysis of the electronic structure of the metal containing catalytic intermediates. While, EPR of low spin (S=1/2) Fe^V have been reported multiple times^[2c] (see Table S1 in the Supporting Information), there are only a few reports where XAS analysis for the proposed Fe^V complexes has been accomplished.^[2a,b,8] XAS characterization requires a high enrichment in the Fe^V species, which is extremely difficult to achieve.^[2a,b] Here, we report XAS characterization of cryogenically trapped [Fe^V=O,(OH) (Pytacn)]²⁺ (2) under conditions of catalytic water oxidation.

Figure 2 shows the Fe K-edge XANES of the initial powder of **1** and its 1 mm solutions in $0.1\,\mathrm{m}$ HNO $_3$ oxidized with 20 equiv of $\mathrm{Ce^{IV}}$ or $\mathrm{NaIO_4}$. Large shifts of the Fe K-edge position were observed indicating the formation of $\mathrm{Fe^V}$ ($\approx +5.26\,\mathrm{eV}$ shift from $\mathrm{Fe^{II}}$, Figure 2). Use of $\mathrm{Ce^{IV}}$ and $\mathrm{NaIO_4}$ produce the same oxidation of **1.** The edge position of the oxidized sample ($\approx 7127.7\,\mathrm{eV}$) is comparable to that reported previously ($\approx 7125.3\,\mathrm{eV}$) for the 70% pure [Fe^V(O) (TAML)]⁻ with an admixture of $\mathrm{Fe^{IV}}$ (Figure S1)^[2b] and exceeds the $\approx 7124.5\,\mathrm{eV}$ reported for 50% content of $\mathrm{Fe^{V}}$ species.^[2a] Pure $\mathrm{Fe^{IV}}$ complexes typically have XANES at

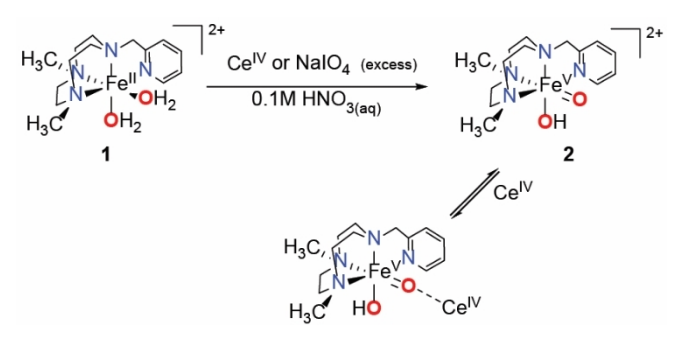


Figure 1. Possible reactive intermediates in water oxidation reaction catalysed by 1.

^[*] R. Ezhov, A. K. Ravari, Y. Pushkar Department of Physics and Astronomy, Purdue University 525 Northwestern avenue, West Lafayette, IN 47906 (USA) E-mail: ypushkar@purdue.edu

Supporting information and the ORCID identification number(s) for the author(s) of this article can be found under: https://doi.org/10.1002/anie.202003278.





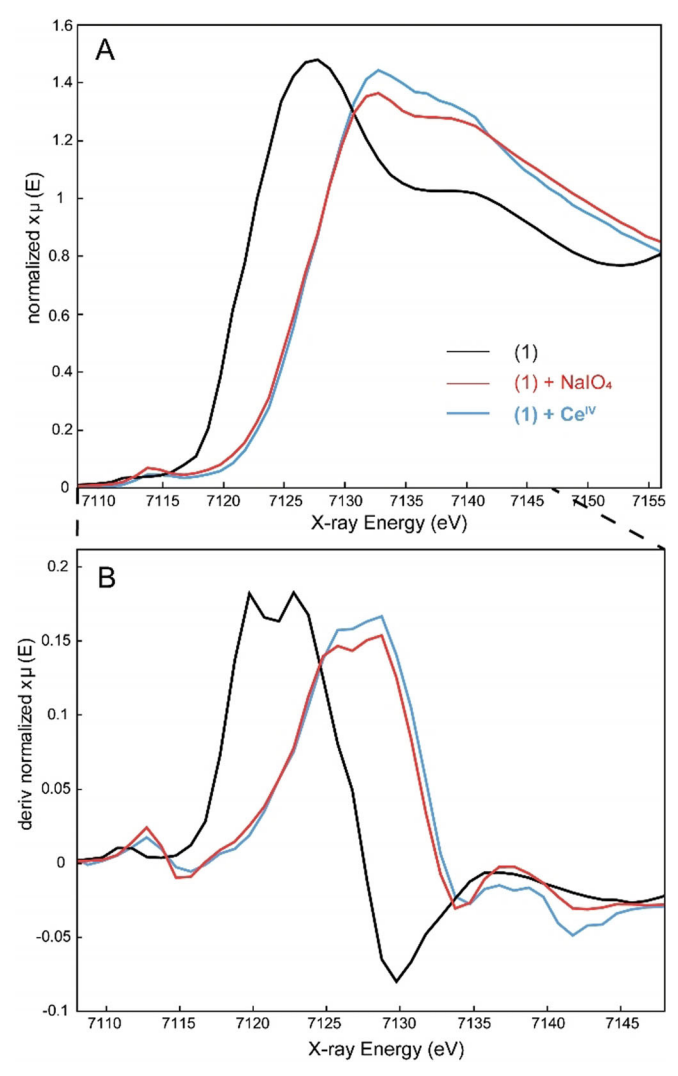


Figure 2. A) Fe K-edge XANES comparison of the spectroscopic characteristics (20 K) of the initial 1 measured as a pellet in a transmission and catalytic mixtures generated by the addition of 20 equiv of Ce^{IV} or $NaIO_4$ oxidant to 1 mm solution of 1 in 0.1 m nitric acid and frozen within 30 s after mixing. B) The corresponding second derivatives of the XANES spectra. The inflection points of the edges allow to quantify change in the oxidation state of the sample.

lower energy^[9] (Figure S1). 5-coordinate [Fe^V(O)(TAML)] also displayed a pronounced pre-edge at \approx 7114 eV due to the oxygen 2p to iron 3d mixing (Figure S1).[2b] This pre-edge, while still present in 2, is significantly less intense (Figure 2). We attribute this differences to the 6-coordinate nature of the $[Fe^{V}=O,(OH)(pytacn)]^{2+}$ intermediate resulting in smaller oxygen 2p to iron 3d mixing needed to observe dipole forbidden 1s to 3d transition.^[10] We have observed a similar effect of the considerable decrease in the pre-edge intensity for the 7-coordinate Ru^V=O complex in comparison to the 5coordinate Ru^V=O with more efficient oxygen 2p and metal d mixing. [6b] XANES data were reproduced over three beamtimes with freshly prepared samples. The following parameters were determined to affect our ability to observe \approx 7127.7 eV edge position: i) freshly dissolved 1 should be used; ii) thorough mixing with the oxidant with simultaneous fast freezing in liquid N_2 should be achieved; iii) any oxidizable impurities should be avoided. DFT predicts $\approx +1.7~{\rm eV}$ redox potential for the formation of the Fe^V in the complex. [5c] Thus, oxidation with the stronger oxidant Ce^{IV} typically gives better results.

Figure 3 compares the EXAFS of the initial powder of 1 and its 1 mm solutions in 0.1m HNO₃ oxidized with 20 equiv of Ce^{IV} or NaIO₄. Two main peaks correspond to the first and second coordination spheres of Fe. In the first coordination sphere of 1, four nitrogens and two oxygens are present (Figure 1). The second coordination sphere is composed of Fe-N-carbon interactions. Table S2 and Figure S2 present the EXAFS fit for the powder sample of 1. Results on bond distances are in good agreement with XRD structures.[11] When the compound is dissolved, two (OTf) anions are quickly exchanged for water ligands. Oxidation with Ce^{IV} or NaIO₄, which both initiate water oxidation and O₂ formation in this catalyst, results in a significant growth of the intensity of the first peak due to the formation of the Fe^V=O fragment at ≈ 1.6 Å (Figure 3). Table S3 and Figure S3 show fits for the oxidized samples of 2. The detected Fe^V=O distance at $\approx 1.60 \text{ Å}$ is in good agreement with DFT calculations for the [Fe^V=O,(OH)(pytacn)]²⁺ intermediate predicting Fe^V=O $\approx 1.63~\mbox{\normalfont\AA}.^{[5c]}$ This distance is also in good agreement with the EXAFS characterization of [Fe^V=O(TAML)] showing $1.58~\mbox{Å}^{[2b]}$ and $\approx\!50\,\%$ \mbox{Fe}^{V} intermediate with $\approx\!1.63~\mbox{Å}.^{[2a]}$ Fe-O bond distance (and edge position) ensures the formulation of the Fe^V=O water oxidation intermediate as the one containing double Fe=O bond character resulting from πinteractions of the p_x and p_y orbitals of the oxo ligand with the higher-energy d_{xz} and d_{yz} orbitals of the d^3 iron center over the alternative oxyl radical Fe^{IV}-O formulation featuring a longer Fe-O bond. [12] Structures of the intermediates formed by oxidation with CeIV or NaIO4 are essentially identical, except for the additional peak at ≈ 3.5 Å apparent distance in samples oxidized with Ce^{IV} (Figure 3). This peak fits well with the Fe···Ce interaction at $\approx 3.7 \text{ Å}$ (Table S3). Complexes of Fe^{IV}=O with cerium were reported with a Fe···Ce distance of $\approx 3.8 \text{ Å}.^{[13]}$

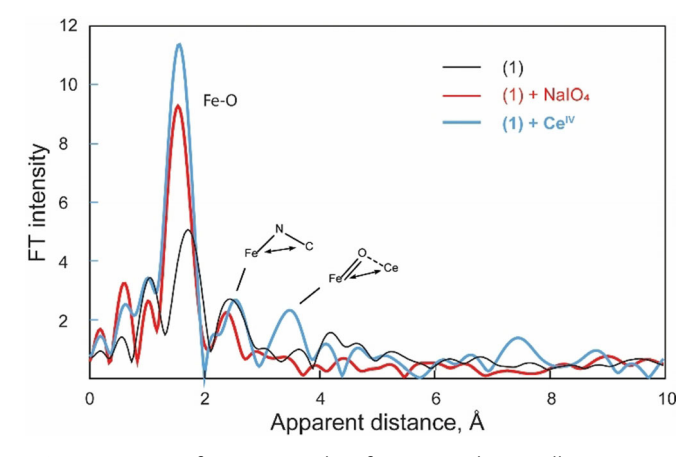


Figure 3. EXAFS of starting powder of 1 measured as a pellet in a transmission and catalytic mixtures generated by the addition of 20 equiv of Ce^{IV} or $ValO_4$ oxidant to 1 mm solution of 1 in $ValO_4$ and frozen within 30 s after mixing.



Combined XANES and EXAFS data indicate at least $\approx 70\%$ content of the [Fe^V=O,(OH)(pytacn)]²⁺ intermediate in the analyzed samples.

While XAS is highly informative for determination of the redox state and molecular geometry, this method cannot confirm the spin state of the oxidized intermediate 2. Earlier DFT analysis concluded that the S=1/2 spin state of 2 is higher in energy by $\approx 15 \text{ kcal mol}^{-1}$. [5c] DFT modelling of the [Fe^V=O,(OH)(Pytacn)]²⁺ complex with cerium showed that spin ordering is not sensitive to Ce binding and the S = 1/2state remains high in energy (Table S4). EPR results are shown in Figures 4 and S4. If [Fe^V=O,(OH)(Pytacn)]²⁺ had a S = 1/2 spin state, its narrow EPR (see Table S1 for g-tensor summary) would be readily detectable even at a low percentage. Reports of high spin (S = 3/2) Fe^V species are extremely rare and their spectra are assumed to vary significantly depending on the system rhombicity.^[14] One study interpreted additional EPR features at $g \approx 3.69$ and 1.96 as Fe^V S = 3/2transitions (Table S1).^[15] EPR samples of 2 generated using Ce^{IV} and periodate exhibit a very broad signal with $g \approx 3.00$, 1.97 and 1.44 components assigned as the S=3/2 EPR of [Fe^V=O,(OH)(Pytacn)]²⁺ (Figures 4, S4) and the admixture of \approx 4.4 (in periodate) and \approx 4.63 (in Ce^{IV}) signals typical of other Fe species. The $g \approx 3.00$, 1.97 and 1.44 signal is extremely temperature dependent; it broadens at $\approx\!20\,K$ and disappears above 30 K. The spectral linewidth indicates extremely fast relaxation. When Ce^{IV} is used as an oxidant, spectral narrowing was observed upon sample storage (Figure S4). We attribute this to a change in the [Fe^V=O,(OH) (Pytacn)]²⁺ environment that affects relaxation. Formation of a complex of 2 with Ce^{IV} cannot be excluded.

Fast relaxation of the detected EPR is in good agreement with the only other EPR report of the Fe^V=N (S=3/2) species.^[16] That first example of Fe^V=N species generated by cryo-photolysis of the corresponding azido-precursors was detected by Raman, EPR and Mössbauer spectroscopy.^[8,16,17] Later, results were re-interpreted via more extensive DFT calculations as the formation of nitrido-Fe^V products with the ground state spin $S=\frac{1}{2}$ and unusual EPR properties.^[8,18]

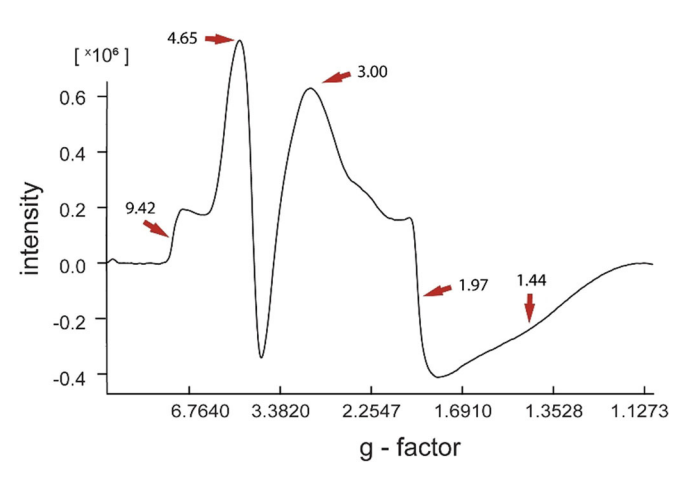


Figure 4. EPR spectra (20 K) of the reactive species generated by addition of 20 equiv of Ce^{IV} to solution of 1 in 0.1 mm nitric acid.

Note that Fe^{IV} (S=2) species are typically EPR undetectable and are unlikely to produce described signals.

Our understanding of the water oxidation mechanisms with the identification of high-valent iron species plays a crucial role in the design of artificial water splitting compounds based on Earth-abundant elements that could be used on the large scale. [5b,13a,19] Until recently, the existence of Fe^V intermediates in transformations of reactive Fe-base coordination complexes was considered elusive. Notably, these types of species have been extensively proposed to be responsible for water oxidation, and selective hydroxylation of alkanes, arenes and olefins catalyzed with aminopyridine iron complexes structurally related to (1).[2d] The majority of Fe^V intermediates in oxidative reactions were observed for iron coordination compounds reacted with peroxo acids in search of suitable oxidizing agents for organic synthesis. [2c,20] All such Fe^V species characterized to date were generated using peroxo acids or H₂O₂ (molecules that have O-O bond fragments and break O-O bond to produce Fe^V=O). Thus, their relevance for O-O bond formation catalysis was not clearly established. Formation of the Fe^V=O intermediate and its high spin (S=3/2) nature in catalytic water oxidation by 1 has been proposed by DFT calculations. [2a,5c,21] Based on the UV/Vis spectrum of the solution, it was concluded that [(pytacn)Fe^{IV}=O,(H₂O)]²⁺ is likely a resting state for this catalyst. Here we showed that under condition of oxidant excess, $[(pytacn)Fe^{V}=O,(OH)]^{2+}$ can be freeze quenched. 2 does not have any pronounced absorption in UV/Vis (Figure S5) and our resonance Raman attempt using 443 nm light was unsuccessful in the recoding spectrum of 2 likely due to poor light absorption/resonance enhancement. This state has a Fe K-edge position consistent with the Fe^V oxidation state and short $\approx 1.60 \text{ Å Fe}^{V}$ =O distance. Previous EPR spectra were reported for low spin (S = 1/2) Fe^V=O intermediates. [2c] However, we did not record the characteristic EPR of the low spin (S=1/2) Fe^V species. This is in agreement with DFT calculations showing that the S=3/2 state is about 15 kcal mol^{-1} more stable than S = 1/2 for [(pytacn)Fe^V=O, $(OH)^{2+}$. [5c] The rate limiting step for O_2 evolution should be a water nucleophilic attack on [(pytacn)Fe^V=O,(OH)]²⁺. The barrier for this process was previously calculated to be $\approx 18.5 \text{ kcal mol}^{-1}$ and the process involved intersystem crossing from the less favorable S = 3/2 pathway to more favorable S = 1/2 pathway.^[5c] While no spectroscopic signatures of the peroxo intermediates have been noted, our data do not contradict the possibility of the water nucleophilic attack on the $[(pytacn)Fe^{V}=O,(OH)]^{2+}$ as the mechanism of the O-O bond formation. Thus, in situ formation of Fe^V=O species in a water oxidation reaction has been experimentally confirmed using EPR and X-ray spectroscopy.

Acknowledgements

We acknowledge the laboratory of Prof. M. Costas for providing catalyst material and for a helpful discussion. This research was supported by NSF, CHE-1900476 (Y.P.). The use of the Advanced Photon Source, an Office of Science User Facility operated by the U.S. Department of Energy (DOE)

Zuschriften





Office of Science by Argonne National Laboratory, was supported by the U.S. DOE under Contract DE-AC02-06CH11357. The PNC/XSD (Sector 20) facilities at the Advanced Photon Source and research at these facilities were supported by the U.S. Department of Energy, Basic Energy Science and the Canadian Light Source. Access to EPR was provided by the Amy Instrumentation Facility, Department of Chemistry, under the supervision of Dr. Michael Everly.

Conflict of interest

The authors declare no conflict of interest.

Keywords: artificial photosynthesis · Fe-based catalysts · highly oxidized species · water oxidation · X-ray spectroscopy

- [1] R. Shang, L. Ilies, E. Nakamura, Chem. Rev. 2017, 117, 9086-
- [2] a) R. X. Fan, J. Serrano-Plana, W. N. Oloo, A. Draksharapu, E. Delgado-Pinar, A. Company, V. Martin-Diaconescu, M. Borrell, J. Lloret-Fillol, E. Garcia-Espana, Y. S. Guo, E. L. Bominaar, L. Que, M. Costas, E. Munck, J. Am. Chem. Soc. 2018, 140, 3916-3928; b) F. T. de Oliveira, A. Chanda, D. Banerjee, X. P. Shan, S. Mondal, L. Que, E. L. Bominaar, E. Munck, T. J. Collins, Science 2007, 315, 835-838; c) O. Y. Lyakin, A. M. Zima, D. G. Samsonenko, K. P. Bryliakov, E. P. Talsi, ACS Catal. 2015, 5, 2702-2707; d) M. Borrell, E. Andris, R. Navratil, J. Roithova, M. Costas, Nat. Commun. 2019, 10, 9.
- [3] a) D. A. Pantazis, ACS Catal. 2018, 8, 9477-9507; b) K. M. Davis, B. T. Sullivan, M. C. Palenik, L. Yan, V. Purohit, G. Robison, I. Kosheleva, R. W. Henning, G. T. Seidler, Y. Pushkar, Phys. Rev. X 2018, 8, 041014; c) Y. Pushkar, K. M. Davis, M. Palenik, J. Phys. Chem. Lett. 2018, 9, 3525-3531.
- [4] a) B. Zhang, L. Sun, Chem. Soc. Rev. 2019, 48, 2216-2264; b) Y. Pineda-Galvan, A. K. Ravari, S. Shmakov, L. Lifshits, N. Kaveevivitchai, R. Thummel, Y. Pushkar, J. Catal. 2019, 375, 1-7; c) D. Erdman, Y. Pineda-Galvan, Y. Pushkar, Catalysts **2017**, 7, 39.
- [5] a) W. C. Ellis, N. D. McDaniel, S. Bernhard, T. J. Collins, J. Am. Chem. Soc. 2010, 132, 10990-10991; b) L. D. Wickramasinghe, R. W. Zhou, R. F. Zong, P. Vo, K. J. Gagnon, R. P. Thummel, J. Am. Chem. Soc. 2015, 137, 13260-13263; c) F. Acuña-Parés, Z. Codolà, M. Costas, J. M. Luis, J. Lloret-Fillol, Chem. Eur. J. 2014, 20, 5696-5707; d) J. L. Fillol, Z. Codola, I. Garcia-Bosch, L. Gomez, J. J. Pla, M. Costas, Nat. Chem. 2011, 3, 807-813.
- [6] a) D. Moonshiram, I. Alperovich, J. J. Concepcion, T. J. Meyer, Y. Pushkar, Proc. Natl. Acad. Sci. USA 2013, 110, 3765-3770; b) D. Lebedev, Y. Pineda-Galvan, Y. Tokimaru, A. Fedorov, N.

- Kaeffer, C. Copéret, Y. Pushkar, J. Am. Chem. Soc. 2018, 140, 451-458; c) N. Planas, L. Vigara, C. Cady, P. Miro, P. Huang, L. Hammarstrom, S. Styring, N. Leidel, H. Dau, M. Haumann, L. Gagliardi, C. J. Cramer, A. Llobet, Inorg. Chem. 2011, 50, 11134-11142.
- [7] L. L. Duan, F. Bozoglian, S. Mandal, B. Stewart, T. Privalov, A. Llobet, L. C. Sun, Nat. Chem. 2012, 4, 418-423.
- [8] N. Aliaga-Alcalde, S. D. George, B. Mienert, E. Bill, K. Wieghardt, F. Neese, Angew. Chem. Int. Ed. 2005, 44, 2908-2912; Angew. Chem. 2005, 117, 2968-2972.
- [9] G. Q. Xue, A. T. Fiedler, M. Martinho, E. Munck, L. Que, Proc. Natl. Acad. Sci. USA 2008, 105, 20615-20620.
- [10] J. Yano, J. Robblee, Y. Pushkar, M. A. Marcus, J. Bendix, J. M. Workman, T. J. Collins, E. I. Solomon, S. DeBeer George, V. K. Yachandra, J. Am. Chem. Soc. 2007, 129, 12989-13000.
- [11] a) A. Company, L. Gómez, M. Güell, X. Ribas, J. M. Luis, L. Que, M. Costas, J. Am. Chem. Soc. 2007, 129, 15766-15767; b) M. Costas, A. K. Tipton, K. Chen, D.-H. Jo, L. Que, J. Am. Chem. Soc. 2001, 123, 6722 – 6723.
- [12] R. Gupta, T. Taguchi, B. Lassalle-Kaiser, E. L. Bominaar, J. Yano, M. P. Hendrich, A. S. Borovik, Proc. Natl. Acad. Sci. USA **2015**, 112, 5319 - 5324.
- [13] a) Z. Codola, L. Gomez, S. T. Kleespies, L. Que, M. Costas, J. Lloret-Fillol, Nat. Commun. 2015, 6, 5865; b) A. Draksharapu, W. Rasheed, J. Klein, L. Que, Angew. Chem. Int. Ed. 2017, 56, 9091-9095; Angew. Chem. 2017, 129, 9219-9223.
- [14] K. L. Kostka, B. G. Fox, M. P. Hendrich, T. J. Collins, C. E. F. Rickard, L. J. Wright, E. Munck, J. Am. Chem. Soc. 1993, 115, 6746 - 6757.
- [15] A. M. Zima, O. Y. Lyakin, K. P. Bryliakov, E. P. Talsi, Chem-CatChem 2019, 11, 5345-5352.
- [16] K. Meyer, E. Bill, B. Mienert, T. Weyhermuller, K. Wieghardt, J. Am. Chem. Soc. 1999, 121, 4859-4876.
- [17] a) W. D. Wagner, K. Nakamoto, J. Am. Chem. Soc. 1988, 110, 4044-4045; b) D. Sellmann, S. Emig, F. W. Heinemann, Angew. Chem. Int. Ed. Engl. 1997, 36, 1734-1736; Angew. Chem. 1997, 109, 1808-1810.
- [18] H. C. Chang, B. Mondal, H. Y. Fang, F. Neese, E. Bill, S. F. Ye, J. Am. Chem. Soc. 2019, 141, 2421-2434.
- [19] a) R. Cao, W. Z. Lai, P. W. Du, Energy Environ. Sci. 2012, 5, 8134-8157; b) M. Yagi, M. Kaneko, Chem. Rev. 2001, 101, 21-35; c) D. G. Nocera, Acc. Chem. Res. 2012, 45, 767 – 776.
- [20] a) M. Borrell, E. Andris, R. Navratil, J. Roithova, M. Costas, Nat. Commun. 2019, 10, 901; b) B. Mondal, F. Neese, E. Bill, S. F. Ye, J. Am. Chem. Soc. 2018, 140, 9531-9544; c) M. Guo, T. Corona, K. Ray, W. Nam, ACS Cent. Sci. 2019, 5, 13-28.
- [21] C. Panda, J. Debgupta, D. D. Diaz, K. K. Singh, S. S. Gupta, B. B. Dhar, J. Am. Chem. Soc. 2014, 136, 12273-12282.

Manuscript received: March 3, 2020 Revised manuscript received: April 15, 2020 Accepted manuscript online: May 5, 2020 Version of record online:





Zuschriften



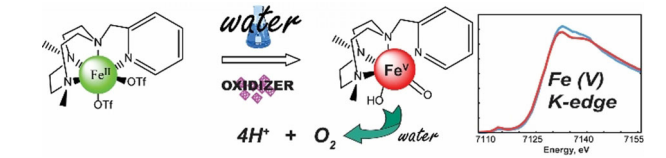
Zuschriften



Artificial Photosynthesis

R. Ezhov, A. K. Ravari,
Y. Pushkar*

Characterization of the $Fe^V = O$ Complex in the Pathway of Water Oxidation



Development of artificial photosynthesis requires efficient water splitting catalysts. The short lived, six coordinated reactive intermediate [Fe^V=O,(OH)(Pytacn)]²⁺ competent in O–O bond formation was trapped. X-ray absorption spectroscopy

(XAS) confirmed Fe V oxidation state and Fe V =O bond at \approx 1.60 Å. EPR and DFT revealed that this is the high spin Fe V complex reacting via water nucleophilic attack to form the O–O bond.